Chemosensors Hot Paper

How to cite: *Angew. Chem. Int. Ed.* **2021**, *60*, 13819–13823
International Edition: doi.org/10.1002/anie.202101004
German Edition: doi.org/10.1002/ange.202101004

A Colorimetric Method for Quantifying *Cis* and *Trans* Alkenes Using an Indicator Displacement Assay

*Stephanie A. Valenzuela[+], Hannah S. N. Crory[+], Chao-Yi Yao[+], James R. Howard, Gabriel Saucedo, A. Prasanna de Silva, and Eric V. Anslyn**

Abstract: *A colorimetric indicator displacement assay (IDA) amenable to high-throughput experimentation was developed to determine the percentage of cis and trans alkenes. Using 96-well plates two steps are performed: a reaction plate for dihydroxylation of the alkenes followed by an IDA screening plate consisting of an indicator and a boronic acid. The dihydroxylation generates either erythro or threo vicinal diols from cis or trans alkenes, depending upon their syn- or anti-addition mechanisms. Threo diols preferentially associate with the boronic acid due to the creation of more stable boronate esters, thus displacing the indicator to a greater extent. The generality of the protocol was demonstrated using seven sets of cis and trans alkenes. Blind mixtures of cis and trans alkenes were made, resulting in an average error of ±2% in the percentage of cis or trans alkenes, and implementing E_2 and Wittig reactions gave errors of ±3%. Furthermore, we developed variants of the IDA for which the color may be tuned to optimize the response for the human eye.*

Optical methods for the rapid screening of enantiomeric excess (*ee*),[1] and in some cases diastereomeric ratio,[2] of stereocenters generated by point-chirality have come to the forefront of high-throughput reaction screening procedures. These optical assays have the goal of lowering the dependence on serial high-performance liquid chromatography and/or nuclear magnetic resonance (NMR) spectroscopy analyses when examining reactions in parallel. However, no optical methods have yet been created for alkene stereochemistry determination. The most common approach to determine alkene stereochemistry is to use ^{1}H NMR coupling constants or known chemical shifts.[3] In other instances, some form of chromatography can be utilized when reference samples are available.[4] In rare cases, reaction-based methods have been reported. For example, Brown and Moerikofer[5] were able to differentiate between *cis* and *trans* alkenes by their rate of hydroboration. In a related endeavor, Li and colleagues[6] exploited *m*-chloroperoxybenzoic acid (*m*-CPBA) to epoxidize unsaturated lipids to identify the location of an olefin, but the method was unable to differentiate stereochemistry.

Osmium tetroxide (OsO_4) is a widely used reagent to dihydroxylate alkenes generating vicinal diols.[7] Under Upjohn conditions, catalytic amounts of OsO_4 can be used to transform alkenes into their respective diols via *syn*-addition.[8] The alkene first undergoes a [3+2] cycloaddition with OsO_4 to form an osmate ester, which is readily hydrolyzed in aqueous systems, commonly yielding the vicinal diol in nearly quantitative yields.[9] In contrast, epoxidation of alkenes using *m*-CPBA followed by ring opening results in the opposite stereochemistry (i.e. *anti*-addition).[10] Thus, by choice of oxidant one can control which diastereomeric diol is created.

While a few host–guest complexes with alkenes as guests have been reported,[11] we postulated that dihydroxylation of an alkene would be an attractive in situ derivatization technique to convert an alkene to a functionality, that is, a vicinal diol, that is more amenable to molecular recognition than an alkene. For example, vicinal diols are well-known to reversibly bind with boronic acids to generate boronate esters, and many groups have used this equilibrium to create chemosensors for carbohydrates.[12]

Previously, our group used the equilibrium between diols and boronic acids to create colorimetric assays that report the *ee* of chiral diols and α-hydroxycarboxylic acids.[13] Using a chiral boronic acid host, these studies exploited an indicator displacement assay (IDA) to generate different colors for the enantiomeric diols. An IDA uses a colorimetric or fluorescent probe, often a pH indicator (I), that has a different optical signal when bound to a host (H) than when free in solution.[14] As shown in Figure 1A, addition of a guest (G) leads to displacement of the indicator, whose optical signal in turn changes.

We sought to exploit the dihydroxylation of alkenes using OsO_4 or *m*-CPBA and an IDA to determine the percentage of *cis* or *trans* alkenes in unknown mixtures or from various reactions. Using 2-pyrrolidinylmethyl-phenylboronic acid as the host (**H**) and pyrocatechol violet as the indicator (**PV**), the resulting 1,2-diols would displace the indicator from the host–indicator complex thereby imparting color changes. Critical to our design was the hypothesis that the diastereomeric diols generated in a stereospecific fashion from the *cis* and *trans* alkenes would have different affinities for **H**. Dihydroxylation of a *cis* alkene using OsO_4 results in an *erythro* diol, which was anticipated to not favor the host–guest complexation due to steric interactions when the R-groups are *cis* to each other in the cyclic boronate ester (Figure 1B).

[*] S. A. Valenzuela,[+] J. R. Howard, G. Saucedo, Prof. E. V. Anslyn
Department of Chemistry, University of Texas at Austin
100 E 24th Street, Norman Hackerman Building (Room 114A)
Austin, TX 78712 (USA)
E-mail: anslyn@austin.utexas.edu
H. S. N. Crory,[+] C.-Y. Yao,[+] Prof. A. P. de Silva, Prof. E. V. Anslyn
School of Chemistry and Chemical Engineering
Queen's University Belfast
Stranmillis Road, Belfast BT9 5AG (UK)
[+] These authors contributed equally to this work.
Supporting information and the ORCID identification number(s) for the author(s) of this article can be found under: https://doi.org/10.1002/anie.202101004.

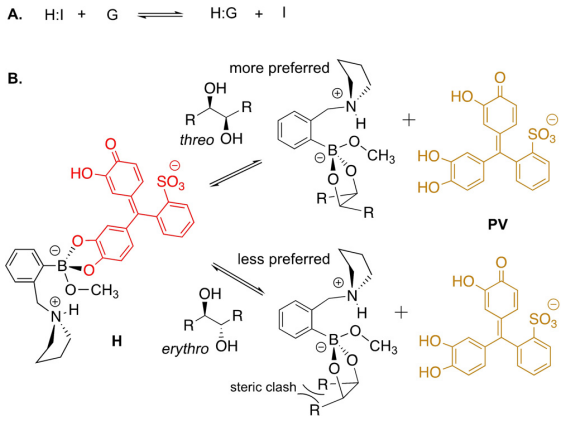

Figure 1. Indicator displacement assay. A) host–indicator (H:I) complex with guest (G) equilibria. B) Representative *threo* and *erythro* diol IDA using pyrocatechol violet (**PV**) as the indicator and 2-pyrrolidinylmethyl-phenylboronic acid (**H**) as the host.

In contrast, when using OsO_4 a *trans* alkene would give a *threo* diol, which places the R-groups *trans* to one another in the formation of the boronate ester. Thus, *trans* alkenes were anticipated to have larger affinities of their corresponding diols than *cis* alkenes, thereby leading to greater displacement of the indicator from the host and in turn larger color changes (Figure 1 B). The use of *m*-CPBA as the oxidant was anticipated to result in the opposite response to diols derived from *cis* and *trans* alkenes.

Prior to developing the IDA protocol depicted in Figure 1, we turned to ^{11}B NMR spectroscopy to verify that **H** preferentially binds with *threo* diols when in competition with *erythro* diols. Using *d*,*l* and *meso*-2,3-butanediol as the guests and **H** (2:1 guest:**H**, 40 mM **H**, MeOH-d_4), the **H** boronate center has a chemical shift of 8.07 ppm. When *meso*-butanediol (*erythro*) was introduced to **H** a new boronate ester resonance emerged downfield at 10.95 ppm, however, the resonance at 8.07 ppm was the dominate peak (Supporting Information, Figure S1). In contrast, upon addition of *d*,*l*-butanediol (*threo*) to **H** the formation of the boronate ester shifted downfield to 10.44 ppm with no remaining peak at 8.07 ppm (Figure S1). When both *d*,*l*- and *meso*-butanediol were allowed to compete for **H** a chemical shift at 10.44 ppm was found, with no signals at 10.95 or 8.07 ppm for the *erythro* diol:**H** complex and **H**, respectively. Additional studies using **G3TH** and **G3ER** (Table 1; 1:1 guest:**H**, 40 mM **H**, 1:1 MeOH-d_4/MeCN-d_3) further supported that **H** preferentially binds with *threo* diols in the presence of *erythro* diols (Figure S2). These studies support our hypothesis that due to the steric interactions shown in Figure 1 B, *threo* diols have a higher affinity for **H** compared to *erythro* diols.

The indicator chosen for the IDA was pyrocatechol violet (**PV**) based upon our previous work for determining the *ee* of chiral diols.[13] To optimize the IDA protocol for the diols derived from alkenes, solvent conditions were first screened. A solvent system of methanol and acetonitrile (1:1, pH 8.4 buffered with *para*-toluenesulfonic acid and Hünig's base) yielded the largest shift in absorbance spectra of **PV** upon binding with **H** (Figure S3). The slightly alkaline pH value for the IDA was selected based upon the pK_a values for *ortho*-amino substituted boronic acids in analogous protic solvents because binding is known to be enhanced by pH values at or above the pK_a values.[15] Using these conditions, a UV/Vis spectrophotometric titration of **PV** with **H** was implemented to determine the binding constant ($K_{\mathbf{H:PV}} = 17.1 \times 10^3\ M^{-1}$, Figure S4) and the optimal concentration of the host and

Table 1: The binding constants, $K_{H:G}$, determined through UV/Vis titration and Os-reaction scheme for the *threo* and *erythro* diols.

Set	Alkenes		Diols	
	trans	*cis*	*threo*	*erythro*
1: R_1, $R_2 = CH_3$	G1T	G1C	G1TH	G1ER
$K_{H:G}$[a]	–	–	0.348	0.057
2: R_1, R_2 = Ph	G2T	G2C	G2TH	G2ER
$K_{H:G}$[a]	–	–	11.1	[b]
3: $R_1 = (CH_2)_7CH_3$ $R_2 = (CH_2)_7COOCH_3$	G3T	G3C	G3TH	G3ER
$K_{H:G}$[a]	–	–	1.38	[b]
4: R_1, $R_2 = (CH_2)_2CH_3$	G4T	G4C	G4TH	G4ER
$K_{H:G}$[a]	–	–	1.10	0.16
5: $R_1 = CH_3$ $R_2 = (CH_2)_2CH_3$	G5T	G5C	G5TH	G5ER
$K_{H:G}$[a]	–	–	2.64[c]	0.29[c]
6: R_1, $R_2 = CH(CH_3)_2$	G6T	G6C	G6TH	G6ER
$K_{H:G}$[a]	–	–	3.72	[b]
7:	G7T	G7C	G7TH	G7ER
$K_{H:G}$[a]	–	–	1.41[c]	0.41[c]

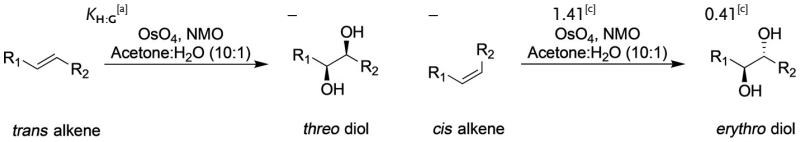

trans alkene — *threo* diol — *cis* alkene — *erythro* diol

[a] $10^3\ M^{-1}$. [b] Negligible measurement. [c] Binding constants determined using the 96-well plate (Supporting Information).

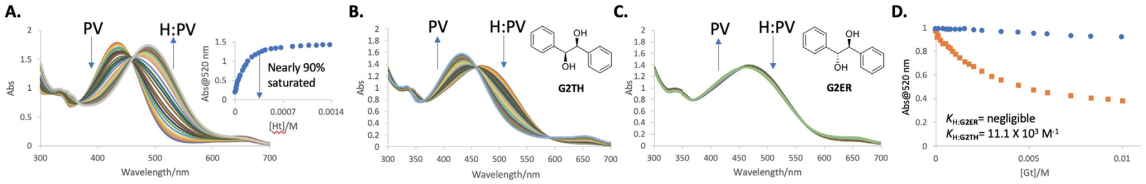

Figure 2. A) UV/Vis titration of host, **H**, into indicator **PV** (0.15 mM). Inset: the change in absorbance at 520 nm with the addition of **H**. [Ht]: host total concentration. B) Representative IDA UV/Vis titration using **G2TH**. C) Representative IDA UV/Vis titration using **G2ER**. D) The difference in absorbance at 520 nm with the addition of **G2TH** (orange) and **G2ER** (blue). [Gt]: total guest concentration. The $K_{H:G2ER}$, binding constant for host **H** is negligible and the $K_{H:G2TH}$, binding constant with **H** is 11.1 (10^3 M^{-1}). All IDAs were analyzed in methanol and acetonitrile (v/v = 1:1, 25 °C, pH 8.4 buffered with 10 mM *para*-toluenesulfonic acid and Hünig's base).

indicator for a subsequent IDA (Figure 2). The concentrations of **PV** (0.15 mM) and **H** (0.4 mM) were chosen because the indicator is approximately 90% saturated with host, and thus would give a large dynamic range in the reversal of the signal upon addition of diols generated from alkenes.

To test the generality of the anticipated preference for *threo* diols, seven sets of isomeric alkenes (Table 1) were subjected to OsO_4, under Upjohn conditions, as a synthetic route to generate both *threo* and *erythro* diols. *Trans* alkenes (or *E*) give *threo* diols whereas *cis* alkenes (or *Z*) lead to *erythro* diols. Using these diols, UV/Vis titration studies were conducted using **H** and **PV** to determine their binding constants using fitting procedures appropriate for IDAs (Figure 2).[16] The *erythro* diols **G2ER**, **G3ER**, and **G6ER** gave minimal signal changes in the IDA, and hence their binding constants were negligible. While **G1ER** and **G4ER** did give signals that were amenable to measuring binding with **H**, the binding constants were approximately seven times smaller than the respective *threo* diol counterparts. Importantly, as revealed by examination of the binding constants in Table 1, the *threo* diol consistently has a stronger affinity to **H** compared to the *erythro* diol for each starting alkene set, further confirming our design hypothesis.

As a specific example, the UV/Vis spectrophotometric titrations using **G2TH** and **G2ER** shown in Figure 2 B,C reveal the preferential binding of **G2TH**. Figure 2 D shows the dramatic difference in the two IDA isotherms (analogous plots for the other diol sets are shown in Figures S5–S10). Further, one visually notices the solution turn from red to yellow as **G2TH** displaces the indicator from the host. In contrast, for **G2ER** no visible color change occurs (Figure 4).

To prepare for the two-step protocol that would involve oxidation using OsO_4 or *m*-CPBA (assuming near quantitative yields[9,10]) in reactions plates followed by IDAs in screening plates, we set out to determine the concentrations for the different diol sets that would give the largest differences in colors. For example, using the **G2TH**/**G2ER** set, the absorbances were determined at 520 nm for different concentrations (Figure S16). The optimal concentration for this diol set was determined to be 10 mM, translating to 10 mM for the **G2T**/**G2C** set. For other alkene sets, different concentrations were used (Figures S17–S22).

For demonstration purposes we focused our testing of the two-step protocol on only the **G2T**/**G2C** and **G3T**/**G3C** sets. **G3** is a fatty acid ester and is therefore of particular interest for lipid analysis. All of the analyses were conducted in triplicates. Prior to the analysis of unknowns and reactions, calibration curves were generated using varying mixtures of each set of alkenes, ranging from 0:100 *cis*/*trans* alkene to 100:0 *cis*/*trans* alkene in increments of 10. For each alkene, the calibration curves were not linear, but instead had a distinct curvature (Figure 3 A; Figure S12). At high percentages of *threo* diols, as created from OsO_4 with *trans* alkenes, the dynamic range of the IDA was large, while changes in the percentages of *threo* diol in an excess of *erythro* diol showed small optical changes. This is as expected, because the *erythro* diol does not displace the indicator, and not until there is a large enough fraction of *threo* diol in the mixture (above $\approx$0.5) does a significant optical response occur.

To explore the diastereoselectivity of the two-step protocol the dihydroxylation of **G2T** and **G2C** was carried out using *m*-CPBA followed by ring opening using KOH (Figure 3 A, and 3B). As would be expected from the opposing stereo-

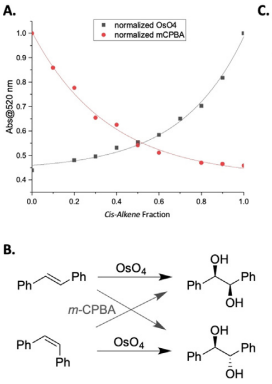

C.

	Abs/ 520 nm	Predict *erythro* diol%	Actual *erythro* diol%
Mixture 1: **G2T/G2C**	0.409	20%	24%
Mixture 2: **G2T/G2C**	0.733	77%	77%
Mixture 3: **G2T/G2C**	0.905	91%	88%
Wittig Reaction	1.021*	19%	23% (NMR)
E_2 Elimination	0.327	<0%	2% (NMR)
Mixture 1: **G3T/G3C**	0.603	50%	54%
Mixture 2: **G3T/G3C**	0.512	26%	27%
Mixture 3: **G3T/G3C**	0.781	79%	81%

Figure 3. A) Representative IDA UV/Vis plate reader calibration curves (520 nm) from screening plates consisting of **G2T** and **G2C** at 10 mM using OsO_4 (black) or *m*-CPBA (red). B) Comparison of the different stereospecificities of OsO_4 and *m*-CPBA. C) First column: UV/Vis plate reader data at 520 nm of the **G2T**/**G2C** blinds and Wittig and E_2 reactions, as well as **G3T**/**G3C** blinds. Second column: predicted % *trans* alkene written as % *erythro* diol from oxidation with OsO_4 using the black calibration curve in part A. Third column: actual percent **G2T**, written again as % *erythro* diol, for the blinds and the Wittig and E_2 reactions (determined by ^{1}H NMR spectroscopy). See Figure S12 for the relevant titration curve for **G3T**/**G3C.** *See Figure S24 for the relevant calibration curve.

specificity of OsO_4 and *m*-CPBA oxidations, the two calibration curves are mirror images across a vertical line at 0.5 fraction of *erythro* diol. Thus, to generate a large enough percentage of *threo* diols for a significant optical response, the proper oxidant needs to be chosen based upon the stereochemistry of the alkene.

We next developed a two-step protocol using two 96 well-plates. We chose OsO_4 as the oxidant and **G2T**/**G2C** and **G3T**/**G3C** as the alkenes (10 and 30 mM respectively). After OsO_4 oxidation, the wells of the reaction plate were quenched with sodium bisulfite and the solutions transferred to and filtered through silica containing 96-well fritted plates to purify the Os-products from $NaHSO_3$ other byproducts. The solvent was removed using a Genevac, and the residues were re-dissolved and transferred to the screening plate containing **H** and **PV**. A blank sample that lacked only the presence of an alkene was subjected to the protocol to serve as a control sample. The control sample confirmed our procedures lacked an absorbance representative of an alkene in the IDA. Furthermore, the control verified our procedures properly removed byproducts during the silica purification steps, showing the absence of residual Os-products. The absorbance of each sample was measured at 520 nm in a UV/Vis plate reader and could be correlated to the percentage of *trans* alkene (Figure 3 B) using the calibration curve in Figure 3 A (black line).

Three "blind" mixtures of **G2T**/**G2C**, as well as synthetically derived mixtures of **G2T**/**G2C** from a Wittig and E_2 reaction were analyzed. The blind mixtures were made by one of the authors and analyzed by a different author without prior knowledge of the percentage of **G2T**. The percentages of **G2T** from the Wittig and E_2 reaction mixtures were verified via ^{1}H NMR spectroscopy (Supporting Information). The calibration curve predicted the **G2T** content in the unknowns to be 20%, 77%, and 91% *erythro* diol, respectively (Figure 3 C), with an average absolute error of ± 2% from the actual values. Additionally, the Wittig and E_2 reaction mixtures were predicted to have 19% and ≈ 0% **G2T**. When verified via ^{1}H NMR spectroscopy the absolute error for the reaction mixtures was ± 3%. As further verification of the two-step protocol, three blind mixtures of **G3T** and **G3C** were generated and taken through the two-step protocol. These were analyzed and determined to be 50%, 26%, and 79% **G3T** with an absolute error of ± 2% from the actual values (Figure 3 C).

We also set out to change the visual color of the solutions containing the host–indicator complex and the liberated free indicator. This allows one to create several different sets of color pairings that may be better suited for one's eye (Figure 4) such that a quick inspection of the color would indicate the predominate alkene stereochemistry within a mixture. Mixing fluorescent indicators have previously been found to optimize sensitivities to pH changes.[17] It is well known that each human has a slightly different ability to distinguish colors.[18] As shown in Figure 4, without an inert food color dye the host–indicator complex (**H:PV**) is red. Addition of a green dye (Wilton food colorings for cakes and icings) makes the solutions orange and addition of a teal dye gives a grey solution. Upon addition of an *erythro* diol (**H:PV** + **G2ER**) the solutions retain their original colors.

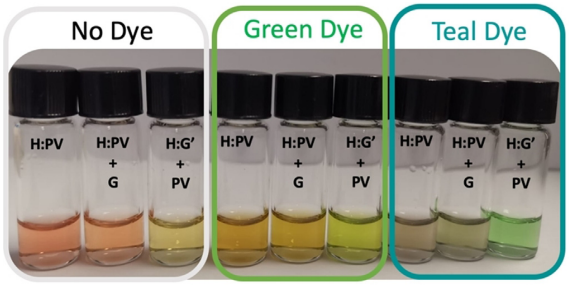

Figure 4. Colorimetric IDA preference. No dye: no inert dye was added. Green Wilton food coloring: 25 µL of green dye was added. Teal dye: 25 µL of each dye was added. **H:PV** host–indicator complex; **H:G'** is the host–*threo* diol complex; **G** represents the *erythro* diol.

However, upon addition of the *threo* diol (**H:PV** + **G2TH**) the solutions turn from burnt red to yellow, orange to lime green, and gray to bright green, respectively (Figure 4). The different colorimetric responses were accomplished with no additional synthesis and can be tuned to alter the appearance of the IDA to best suit one's eye. Interestingly, for the authors, most felt the teal background dye gave the most obvious response to the *erythro* diol, but for others, different colors were optimal.

In conclusion, we have reported the first optical approach for determining the percentage of *cis* and *trans* alkenes that is amenable to a high-throughput workflow. We successfully used two synthetic techniques to dihydroxylate alkenes, with opposite stereospecificity, in 96-well plates. The resulting diastereomeric 1,2-diols were analyzed using an IDA via UV/Vis spectroscopy in 96-well plates to determine the percent of *trans* or *cis* alkene. We were successful at determining the percentage of blind mixtures of alkenes, as well as two reactions as unknowns, with an average error consistently less than ± 3%. Furthermore, we explored the general utility of an IDA to impart different colors for the alkenes with no additional synthetic effort. This study gives chemists another tool to determine the percentage of *cis* and *trans* alkenes—one that is amenable to a high-throughput experimentation workflow because of the use of parallel analysis in plates instead of the use of serial NMR spectroscopy or chromatography.

Acknowledgements

We would like to thank the Brodbelt research group, University of Texas at Austin, for inspiring our group to tackle this challenge. For this project, S.A.V. was funded primarily through the NSF Graduate Research Fellowship Program: DGE-1610403. Additionally, we would like to thank and recognize the University of Texas at Austin's Mass Spectrometry Facility for their help and the NMR facilities for Bruker AVANCE III 500: NIH Grant Number 1 S10 OD021508-01. This project was primarily funded through the NSF GOALI Grant Number: 1665040. Furthermore, E.V.A. recognizes support from the Welch Regents

Chair (1-0046). We would like to acknowledge the Department of Employment and Learning of Northern Ireland and China Scholarship Council. The authors recognize Queen's University Belfast and Prof. P. Nockemann for their contributions to this collaboration.

Conflict of interest

The authors declare no conflict of interest.

Keywords: alkene stereochemistry · colorimetric assays · dihydroxylation · high-throughput screening · host–guest systems

[1] B. T. Herrera, S. L. Pilicer, E. V. Anslyn, L. A. Joyce, C. Wolf, *J. Am. Chem. Soc.* **2018**, *140*, 10385 – 10401.
[2] a) B. T. Herrera, S. R. Moor, M. McVeigh, E. K. Roesner, F. Marini, E. V. Anslyn, *J. Am. Chem. Soc.* **2019**, *141*, 11151 – 11160; b) Z. A. De los Santos, S. MacAvaney, K. Russell, C. Wolf, *Angew. Chem. Int. Ed.* **2020**, *59*, 2440 – 2448; *Angew. Chem.* **2020**, *132*, 2461 – 2469.
[3] a) Y. Chi, T. J. Peelen, *Org. Lett.* **2005**, *7*, 3469 – 3472; b) D. P. Iwaniuk, C. Wolf, *J. Org. Chem.* **2010**, *75*, 6724 – 6727; c) A. Shundo, J. Labuta, J. P. Hill, S. Ishihara, K. Ariga, *J. Am. Chem. Soc.* **2009**, *131*, 9494 – 9495; d) W. D. G. Brittain, B. M. Chapin, W. Zhai, V. M. Lynch, B. R. Buckley, E. V. Anslyn, J. S. Fossey, *Org. Biomol. Chem.* **2016**, *14*, 10778 – 10782.
[4] a) K. Ebinger, H. N. Weller, *J. Chromatogr. A* **2013**, *1272*, 150 – 154; b) N. Joshi, B. Dhamarlapati, A. Pillai, J. Paulose, J. Tan, L. E. Blue, J. Tedrow, B. Farrell, *J. Chromatogr. A* **2018**, *1538*, 108 – 111.
[5] H. C. Brown, A. W. Moerikofer, *J. Am. Chem. Soc.* **1963**, *85*, 2063 – 2065.
[6] Y. Feng, B. Chen, Q. Yu, L. Li, *Anal. Chem.* **2019**, *91*, 1791 – 1795.
[7] a) K. B. Sharpless, K. Akashi, *J. Am. Chem. Soc.* **1976**, *98*, 1986 – 1987; b) Lemieux-Johnson Oxidation: R. Pappo, D. S. Allen, Jr., R. U. Lemieux, W. S. Johnson, *J. Org. Chem.* **1956**, *21*, 478 – 479; c) J. K. Cha, N.-S. Kim, *Chem. Rev.* **1995**, *95*, 1761 – 1795; d) A. Français, O. Bedel, A. Haudrechy, *Tetrahedron* **2008**, *64*, 2495 – 2524; e) J. Eames, H. Mitchell, A. Nelson, P. O'Brien, S. Warren, P. Wyatt, *J. Chem. Soc. Perkin Trans. 1* **1999**, 1095 – 1104.
[8] a) N. A. Milas, S. Sussman, *J. Am. Chem. Soc.* **1936**, *58*, 1302 – 1304; b) V. VanRheenen, R. C. Kelly, D. Y. Cha, *Tetrahedron Lett.* **1976**, *17*, 1973 – 1976.
[9] U. Pidun, C. Boehme, G. Frenking, *Angew. Chem. Int. Ed. Engl.* **1996**, *35*, 2817 – 2820; *Angew. Chem.* **1996**, *108*, 3008 – 3011.
[10] a) N. N. Schwartz, J. H. Blumbergs, *J. Org. Chem.* **1964**, *29*, 1976 – 1979; b) J. L. García Ruano, C. Fajardo, A. Fraile, R. M. Martín, *J. Org. Chem.* **2005**, *70*, 4300 – 4305.
[11] a) B. Esser, J. M. Schnorr, T. M. Swager, *Angew. Chem. Int. Ed.* **2012**, *51*, 5752 – 5756; *Angew. Chem.* **2012**, *124*, 5851 – 5855; b) D. Fong, S. X. Luo, R. S. Andre, T. M. Swager, *ACS Cent. Sci.* **2020**, *6*, 507 – 512; c) R. W. Pow, W. Xuan, D. L. Long, N. L. Bell, L. Cronin, *Chem. Sci.* **2020**, *11*, 2388 – 2393.
[12] a) G. Springsteen, B. Wang, *Tetrahedron* **2002**, *58*, 5291 – 5300; b) X. Sun, B. M. Chapin, P. Metola, B. Collins, B. Wang, T. D. James, E. V. Anslyn, *Nat. Chem.* **2019**, *11*, 768 – 778; c) Y. Suzuki, A. Ikeda, K. Ohno, T. Fujihara, T. Sugaya, K. Ishihara, *J. Org. Chem.* **2020**, *85*, 9680 – 9693; d) S. D. Bull, M. G. Davidson, J. N. H. van den Elsen, J. S. Fossey, T. A. Jenkins, Y. B. Jiang, Y. Kubo, F. Marken, K. Sakurai, J. Zhao, T. D. James, *Acc. Chem. Res.* **2013**, *46*, 312 – 326; e) W. Zhai, X. Sun, T. D. James, J. S. Fossey, *Chem. Asian J.* **2015**, *10*, 1836 – 1848.
[13] a) L. Zhu, Z. Zhong, E. V. Anslyn, *J. Am. Chem. Soc.* **2005**, *127*, 4260 – 4269; b) S. H. Shabbir, R. J. Clinton, E. V. Anslyn, *Proc. Natl. Acad. Sci. USA* **2009**, *106*, 10487 – 10492.
[14] a) R. N. Dsouza, U. Pischel, W. M. Nau, *Chem. Rev.* **2011**, *111*, 7941 – 7980; b) L. E. Santos-Figueroa, M. E. Moragues, E. Climent, A. Agostini, R. Martínez-Máñez, F. Sancenón, *Chem. Soc. Rev.* **2013**, *42*, 3489 – 3613.
[15] X. Sun, B. M. Chapin, P. Metola, B. Collins, B. Wang, T. D. James, E. V. Anslyn, *Nat. Chem.* **2019**, *11*, 768 – 778.
[16] K. A. Connors, *Binding Constants, The Measurement of Molecular Complex Stability*, Wiley, New York, **1987**, pp. 141 – 168.
[17] G. Gabor, D. R. Walt, *Anal. Chem.* **1991**, *63*, 793 – 796.
[18] a) J. Neitz, M. Neitz, G. H. Jacobs, *Vis. Res.* **1993**, *33*, 117 – 122; b) J. A. Endler, *Biol. J. Linn. Soc.* **1990**, *41*, 315 – 352.

Manuscript received: January 21, 2021
Revised manuscript received: March 12, 2021
Accepted manuscript online: March 15, 2021
Version of record online: May 12, 2021

